4.4 Double exposure by means of a birefringent plate

In the previous sections three coherent multiple imaging techniques were discussed, where the final image could be obtained by a coherent superposition of two fields. In this section a fourth technique will be discussed theoretically, where the final image is resulted of two incoherent fields [69].

4.4.1 Geometrical Optics Model

The displacement of the focus point when a plane parallel plate is placed behind a lens is a well-known fact. Based on geometrical optics considerations, the shift of focus (Δf) is:

$$\Delta f = d \cdot \left(1 - \frac{cos(\alpha)}{\sqrt{n^2 - sin^2(\alpha)}}\right), \tag{4.5}$$

where d is the thickness, n is the refractive index of the plate and α is the incident angle.

As the focus shift depends on the refractive index, we expect that using a birefringent plane-parallel plate instead of the isotropic plate, two focal points will appear (o/e images): one created by the ordinary, and the other created by the extraordinary ray. We deal with the case when the optical axis is perpendicular to the surface's normal (see Fig. 4.11). The intensity distribution after the birefringent plate in the vicinity of the focal point was calculated using scalar wave optics model. The angle dependent phase error introduced by the thin plane-parallel plate is:

$$\phi(\alpha) = k \cdot (n_2 cos(\beta) - n_1 cos(\alpha)), \tag{4.6}$$

where β is the refractive angle inside the plate, n_2 is the refractive index of the plate and n_1 is the refractive index of the environment (we assume that the system is in vacuum, hence n_1=1). Let us introduce a new variable: $s = sin(\alpha)/2$, and let us expand $f(s)$ in terms of a power series in s. By means of this new variable, the defocus can be represented by a single term.

$$\phi(s) = k \cdot d(n_2 - n_1)\left(1 + \frac{2n_1}{n_2}s^2 + 2(n_1 + n_2)\frac{n_1^2}{n_2^3}s^4 + 4(n_1 + n_2)\frac{n_1^4}{n_2^5}s^6\right) \tag{4.7}$$

The term in s^2 represents the defocus introduced by the slab, while the term in s^4 represents the primary spherical aberration. Using the scalar theory, the intensity in the focal region is [70, 71]:

$$I(u,v) = \left| \int_0^{\alpha_0} \sqrt{cos(\alpha)} \cdot e^{i\phi(\alpha)} J_0\left(\frac{v sin(\alpha)}{sin(\alpha_0)}\right) \cdot e^{-\frac{1}{2}iu\frac{sin^2(\alpha/2)}{sin^2(\alpha_0/2)}} \cdot sin(\alpha) d\alpha \right|^2 , \qquad (4.8)$$

where $u = 4kzsin^2(\alpha_0/2)$, $v = krsin(\alpha_0)$, and α_0 is the semi-angle of convergence. Using the new variable, the intensity distribution on the optical axis is:

$$I(u) = \left| \int_0^{sin(\alpha_0/2)} B(s) \cdot P(s) \cdot e^{-\frac{1}{2}iu\frac{s^2}{sin^2(\alpha_0/2)}} sds \right|^2 , \qquad (4.9)$$

where $B(s) = 4(2s^2 - 1)^{1/4}$ and $P(s) = e^{i\phi(s)}$ is the wavefront aberration function.

During the calculation we assumed that the extraordinary refractive index is constant and does not depend on the direction of the ray. We have two reasons for using this simplification. On the one hand we use only part of the refractive index ellipsoid which is determined by the numerical aperture of the projection lens. In case of NA=0.3 (α_0=18°) the maximum refractive index difference inside the illuminated cone is 0.0012 for MgF_2 and 0.014 for calcite, which is smaller than 10% of the difference between the ordinary and extraordinary refractive indexes for both cases. On the other hand, distortions introduced by the non-cylindrical symmetry of the system can also be addressed, if instead of a single "thick" slab, we apply a slab containing several plates, for which the optical axes are rotated against each other.

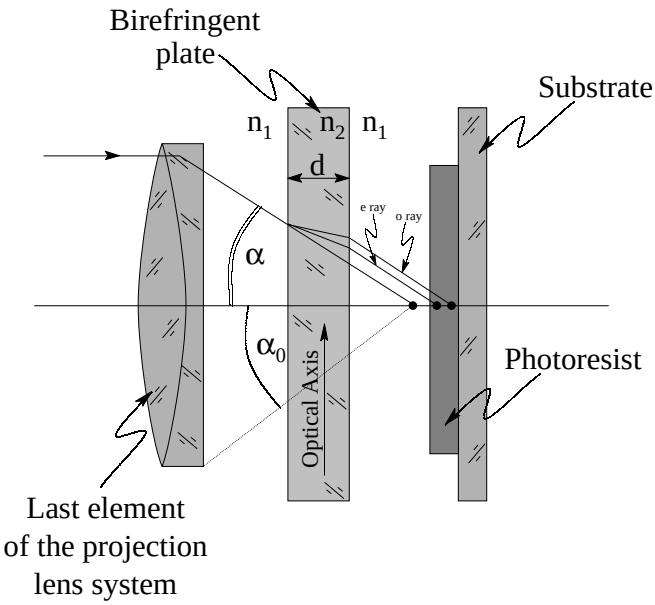

Figure 4.11: Focusing through a birefringent plate.

Figure 4.12 shows the normalized intensity distributions for MgF_2 and calcite slabs using different plate thickness. The numbers adjacent to the peaks display the intensity maxima comparing with the case when no birefringent plate is used and the intensity maximum is 1. The insets depict the two-dimensional intensity distribution on the optical axis. The solid thin lines show the images created by the ordinary rays, the thin

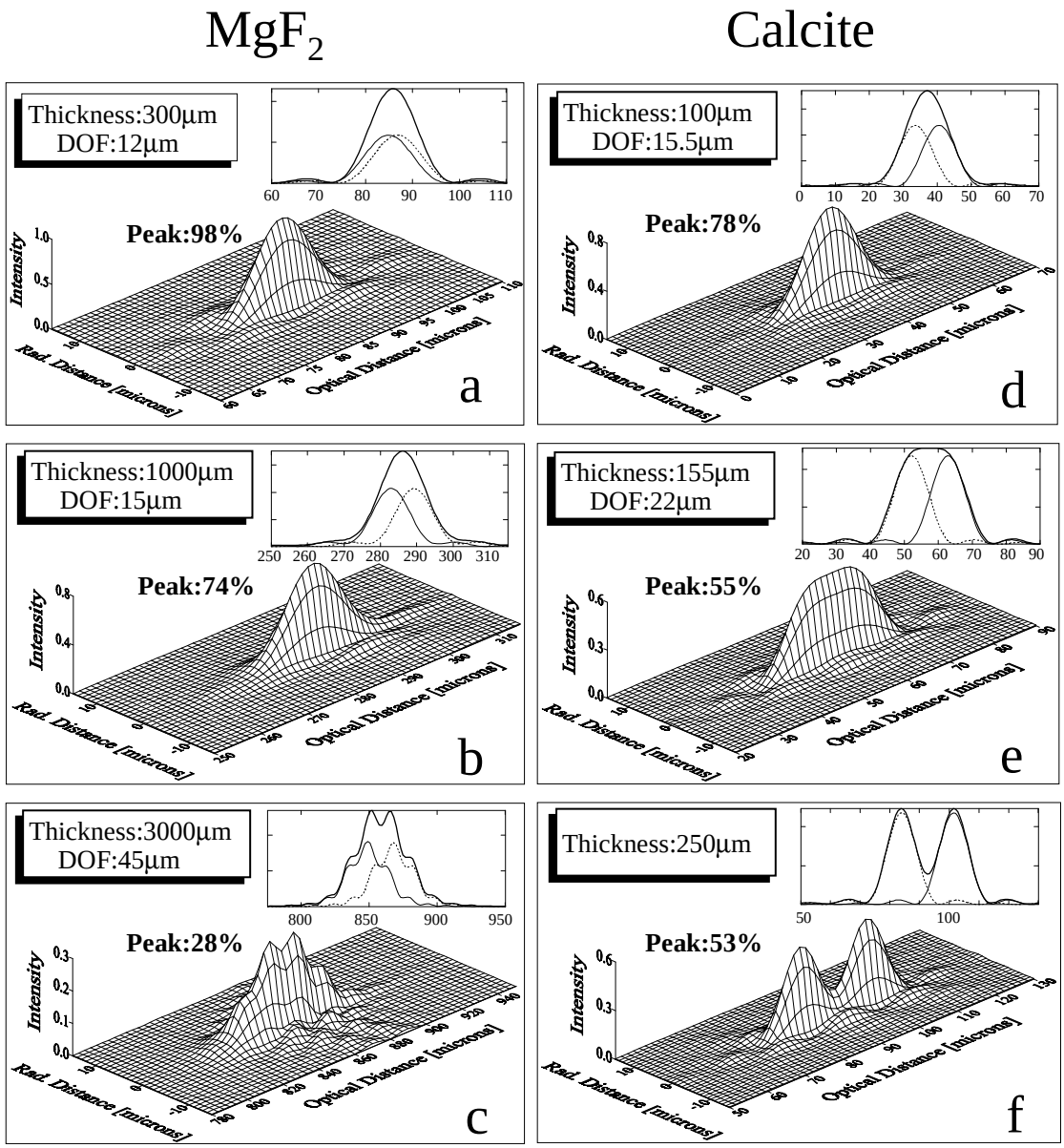

Figure 4.12: Calculated intensity distribution in the vicinity of the focus point using a birefringent slab inserted behind the lens.

dashed lines show the images created by the extraordinary rays, while the thick solid lines depict the total intensity distributions. Since MgF_2 is a positive uniaxial crystal ($n_o < n_e$), the image created by the ordinary ray precedes the image generated by the extraordinary ray. Calcite is a negative uniaxial crystal, hence the order of the o/e images are exchanged. The refractive index difference between the ordinary and the extraordinary rays significantly determines the final image profile. Calcite is a strongly birefringent material (n_o=1.656, n_e=1.485, Δn=0.171), hence a thin, almost 155 μm

plate is sufficient. In Fig. 4.12-e the separation of the o/e images almost equals their DOF, hence the DOF of the final image is twice as large as the separated images. Using a thinner plate the o/e images came closer to each other, hence the DOF enhancement is not significant. In case of a thick slab, the o/e images are separated and DOF enhancement cannot be obtained. MgF_2 is a slightly birefringent material (n_o=1.378, n_e=1.39, Δn=0.012), therefore a thicker plate is necessary to reach the same effect. Figures 4.12-a,b,c show the intensity distributions using MgF_2 plates with different thickness. Since a thick slab beyond the projection lens causes undesirable aberration effects (see Fig. 4.12-c), the intensity distributions are not as smooth as they were using calcite plate. The optimum thickness of the MgF_2 plate was around 1000μm (see Fig. 4.12-b). Hence the application of a thin but strongly birefringent material is a better candidate than that of a slightly birefringent but thick plate, since aberrations proportional to the thickness of the plate become insignificant. Since a birefringent plate located between the projection lens and the wafer cannot be defined in the present microlithographic simulation tools, we plan to evaluate the process experimentally.